Drug Design, Development and Therapy

Dovepress
open access to scientific and medical research

Open Access Full Text Article

ORIGINAL RESEARCH

Network Pharmacology and Experimental Validation to Explore the Effect and Mechanism of Kanglaite Injection Against Triple-Negative Breast Cancer

Mei Zhao[1,2], Lijuan Fu[1,2], Panling Xu[1,2], Ting Wang[1,2], Ping Li[1,2]

[1]Department of Chinese Integrative Medicine Oncology, The First Affiliated Hospital of Anhui Medical University, Hefei, People's Republic of China; [2]Department of Integrated Traditional Chinese and Western Medicine, Anhui Medical University, Hefei, People's Republic of China

Correspondence: Ping Li, Department of Chinese Integrative Medicine Oncology, The First Affiliated Hospital of Anhui Medical University, No. 120 Wanshui Road, Hefei, 230032, Anhui, People's Republic of China, Email liping1964@ahmu.edu.cn

Purpose: Kanglaite injection (KLTi), made of Coix seed oil, has been shown to be effective in the treatment of numerous cancers. However, the anticancer mechanism requires further exploration. This study aimed to investigate the underlying anticancer mechanisms of KLTi in triple-negative breast cancer (TNBC) cells.

Methods: Public databases were searched for active compounds in KLTi, their potential targets and TNBC-related targets. KLTi's core targets and signaling pathways were determined through compound-target network, protein–protein interaction (PPI) network, Gene Ontology (GO) and Kyoto Encyclopedia of Genes and Genomes (KEGG) pathway enrichment analysis. Molecular docking was carried out to predict the binding activity between active ingredients and key targets. In vitro experiments were conducted to further validate the predictions of network pharmacology.

Results: Fourteen active components of KLTi were screened from the database. Fifty-three candidate therapeutic targets were selected, and bioinformatics analysis was performed to identify the top two active compounds and three core targets. GO and KEGG enrichment analyses indicated that KLTi exerts therapeutic effects on TNBC through the cell cycle pathway. Molecular docking results showed that the main compounds of KLTi exhibited good binding activity to key target proteins. Results from in vitro experiments showed that KLTi inhibited proliferation and migration of TNBC cell lines 231 and 468, induced apoptosis, blocked cells in the G2/M phase, downregulated the mRNA expression of seven G2/M phase-related genes cyclin-dependent kinase 1 (CDK1), cyclin-dependent kinase 2 (CDK2), and checkpoint kinase 1 (CHEK1), cell division cycle 25A (CDC25A), cell division cycle 25B (CDC25B), maternal embryonic leucine zipper kinase (MELK), and aurora kinase A (AURKA), as well as downregulated CDK1 protein expression and up-regulated protein expression of Phospho-CDK1.

Conclusion: By utilizing network pharmacology, molecular docking, and in vitro experiments, KLTi was confirmed to have anti-TNBC effects by arresting cell cycle and inhibiting CDK1 dephosphorylation.

Keywords: Kanglaite injection, triple-negative breast cancer, network pharmacology, cell cycle, CDK1

Introduction

With approximately 2.3 million new cases in 2020, breast cancer (BC) has become the most commonly diagnosed cancer worldwide.[1] Simultaneously, the mortality rate of BC is increasing annually, accounting for approximately 6.9% of all cancer-related deaths.[1,2] Triple-negative breast cancers (TNBCs) are defined as tumors lacking the expression of estrogen receptors (ER), progesterone receptors (PR), and human epidermal growth factor receptor-2 (HER2), and account for 15–20% of all BCs.[3–5] As an aggressive disease, TNBC is characterized by high recurrence and metastasis rates, short survival, and afflicts younger women.[6] Treatment options are limited; chemotherapy remains the first choice for patients

Received: 22 November 2022
Accepted: 16 March 2023
Published: 23 March 2023

with advanced TNBC with severe side effects and prevalent drug resistance. For this reason, alternative treatment options for TNBC need to be identified.

Kanglaite injection (KLTi) is mainly composed of Coix seed oil, which is extracted from the Coix seed, and KLTi was approved by the National Medical Products Administration in 2010 (National Medical License No.: Z14021231). KLTi has been used clinically to treat numerous cancers, including non-small cell cancer,[7] gastric cancer,[8] pancreatic cancer,[9] and BC.[10,11] Preclinical studies have identified that KLTi exerts antitumor effects by regulating the PI3K/AKT/mTOR signaling pathway and the miR-205/S1PR1 axis.[12,13] However, the exact anti-tumor mechanisms are still not fully understood and deserve further exploration.

Bioinformatics databases serve as the basis for network pharmacology, which attempts to systematically explain the mechanisms of action of traditional Chinese medicine (TCM) through network analysis of drugs, genes, compounds, and diseases.[14] Network pharmacology operates by finding the active ingredients of drugs, predicting their targets, and then combining them with disease targets to build a visualized "drug-target-disease" network.[15] On this basis, multiple possible targets and pathways for drug action in diseases are further explored. The study of multi-target pathways is at the core of network pharmacology and is currently used to study the mechanism of action of herbal medicines, their compounding, and the development of new drugs, especially in cancer therapy.[16] To our knowledge, there have been no studies using network pharmacology to study the molecular mechanism of KLTi in TNBC.

Therefore, we used a network pharmacology approach to predict the mechanism of the anti-TNBC effect of KLTi. Subsequently, we performed molecular docking validation and in vitro experiments to evaluate the anti-TNBC effect of KLTi and initially validated its molecular mechanism of action. The flow chart of the study is shown in Figure 1. This study aimed to explore the anti-TNBC effect of KLTi from another perspective and to elucidate its mechanisms.

Materials and Methods

Searching for Active Compounds and Potential Targets of KLTi

The active components of KLTi were identified by a literature review.[13,17] We then identified the total chemical composition of Coix lacryma-jobi, the main component of KLTi, from the Traditional Chinese Medicine Database and Analysis Platform (TCMSP) (https://tcmsp-e.com/tcmsp.php) and selected the active compounds based on the ADME (absorption, distribution, metabolism, and excretion) screening principle.[18] Since KLTi is administered intravenously, screening for oral bioavailability (OB) specific to oral drugs is not required, and the condition of drug-likeness (DL) was set at $\geq$0.18.[17]

We obtained the canonical simplified molecular input line entry specification (SMILES) of active compounds from the PubChem database (https://pubchem.ncbi.nlm.nih.gov/). The SMILES were inputted into the Swiss Target Prediction database (http://swisstargetprediction.ch/) for potential targets, which were screened out with a probability >0.[19] The information of compounds was also inputted into DrugBank (https://go.drugbank.com/) and TargetNet (http://targetnet.scbdd.com/) to obtain more potential targets.[20,21] The predicted multi-target information of the compounds and the obtained data were used to construct a compound-target network using Cytoscape 3.9.1.[22] The nodes in this network represent the active compounds and targets of KLTi, and the edges illustrate the interactions and internal relationships between the active compounds and targets.

Identification of TNBC-Related Targets

Using the GEO database (https://www.ncbi.nlm.nih.gov/geo),[23] differentially expressed genes (DEGs) were identified in cancerous and healthy tissue of TNBC patients by searching "triple negative breast cancer" or "TNBC" as keywords, and screening "Homo sapiens" and "Expression profiling by array" as qualifiers. The dataset GSE38959 was selected and analyzed using GEO2R. The DEGs of TNBC were selected based on adjusted p-value <0.05 and |log2FC|>1.

Potential Targets of KLTi for the Treatment of TNBC

Venny 2.1.0 (https://bioinfogp.cnb.csic.es/tools/venny/index.html) was used to screen for overlapping KLTi compound targets and TNBC-related targets. The overlapping genes were used to construct networks and perform additional

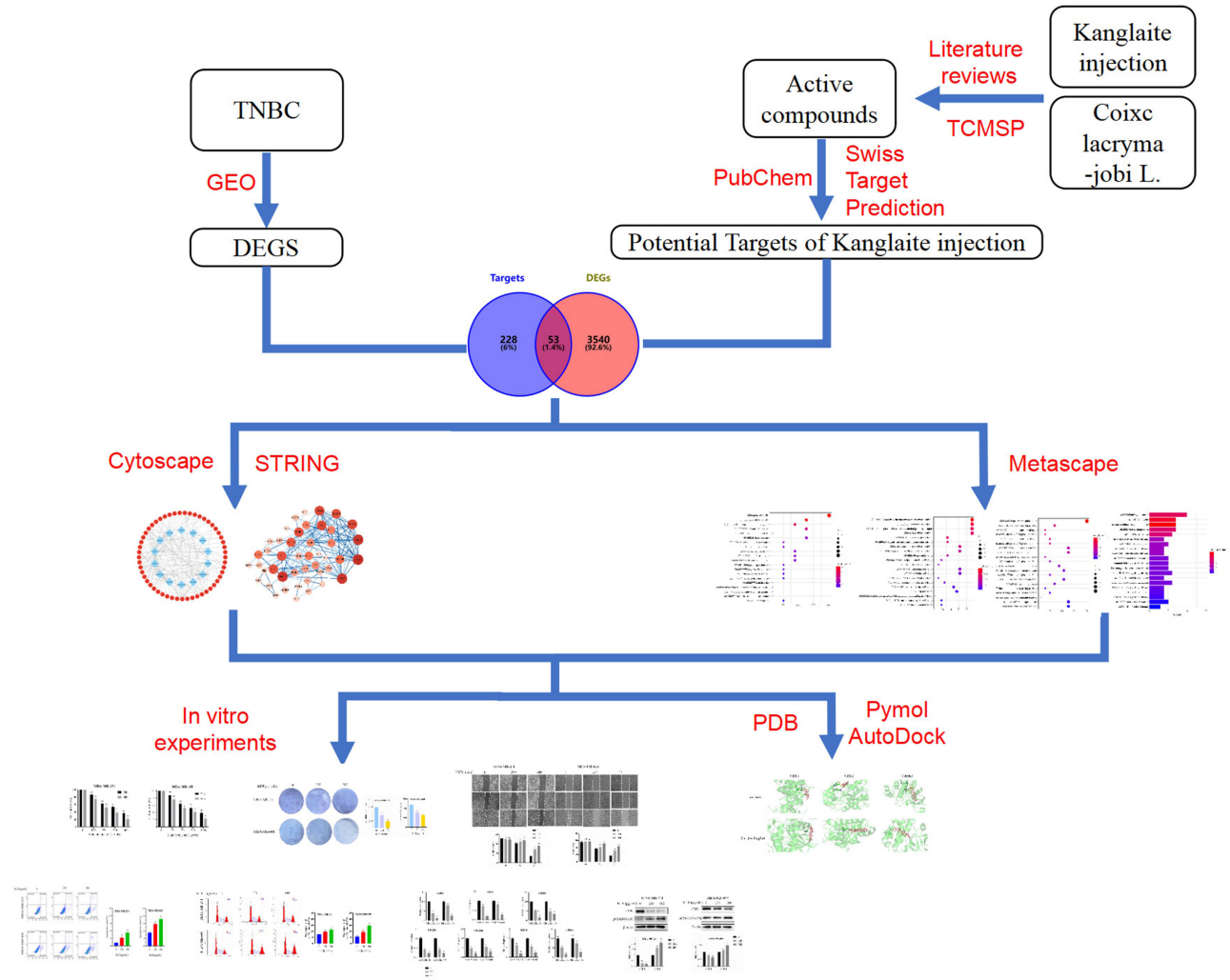

Figure 1 The flow chart of the study.

analyses. Cytoscape 3.9.1 was used to construct a compound-target network of KLTi against TNBC. The relationships between compounds and targets were analyzed based on Cytoscape's built-in network analysis tool, focusing on the degree of connectivity. The higher the degree value, the higher the importance of biological function.

Protein–Protein Interaction (PPI) Data

The analysis was performed using overlapping genes in the STRING database (https://cn.string-db.org, version 11.5, updated August 12, 2021) to clarify the interaction relationships between the functional proteins.[24] We set the screening criteria as "Homo sapiens" and "medium confidence" and hid disconnected nodes in the network to obtain the PPI network. The TSV format files downloaded from the STRING database were then imported into Cytoscape 3.9.1. The key topological parameter, degree, describes the most important nodes in the network; higher quantized values of topological parameters indicate a greater importance of nodes.

Pathway Enrichment Analysis

The Gene Ontology Consortium (GO) and Kyoto Encyclopedia of Genes and Genomes (KEGG) analyses of overlapping genes were performed using Metascape (https://metascape.org/).[25–27] GO analysis of biological processes (BP), molecular function (MF), cellular component annotation (CC), and enrichment analysis of KEGG pathways were performed

based on p-values <0.05. Twenty GO and KEGG processes with significant differences were screened out, and the results were visualized and analyzed using the bioinformatics website (http://www.bioinformatics.com.cn/).

Molecular Docking

The main active components of KLTi were chosen for molecular docking of the core targets. Molecular structures of the active ligand components are available at PubChem (http://pubchem.ncbi.nlm.nih.gov/). The Protein Data Bank (PDB) database (https://www.rcsb.org/)[28] was used to obtain 3D structure formats for the targets. Protein dehydration and ligand removal were performed using PyMOL 2.5 software (Schrodinger, USA). Target protein hydrogenation and charge calculations were performed using AutoDock4.2.6 (Scripps Research, USA), and docking was performed using AutoDockTools 1.5.7 (Scripps Research, USA). Visualization of docking results was performed using PyMOL 2.5 (Schrodinger, USA).

Cell Lines and Reagents

Human TNBC cell lines MDA-MB-231 (231) and MDA-MB-468 (468) were obtained from the Cell Bank of the Chinese Academy of Sciences (China) and were maintained in Dulbecco's modified eagle medium (BI, USA) supplemented with 10% fetal bovine serum (BI, USA) and 1% penicillin-streptomycin solution (100×, Beyotime, China) and incubated at 37°C in a humidified incubator containing 5% carbon dioxide. KLTi was purchased from Zhejiang Kanglaite Pharmaceutical Co., Ltd (China).

Cell Viability Assay

Enhanced Cell Counting Kit-8 (CCK-8) (Beyotime, China) was used to measure cell viability, and 231 and 468 cell suspensions were seeded in 96-well plates at 2000 cells per well with 100 ul and incubated for 24 h. Cells were then treated with KLTi (0, 125, 250, 500, and 1000 ug/mL) and incubated at 37°C for 48 or 72 h. Afterwards, an absorbance measurement at 450 nm (BIO-TEK, Synergy H1, USA) was performed after cells were incubated with CCK-8 medium for 1 h. The experiments were performed in triplicate.

Colony Formation Assay

Suspensions of 231 and 468 cells were inoculated into 6-well plates at a density of 1000 cells/well. The cells were treated with different doses of KLTi. After 10 days of incubation, when the colonies contained more than 50 cells, the plates were washed three times with phosphate-buffered saline (PBS), then fixed with paraformaldehyde and stained with crystal violet. Colonies were counted using a microscope (Olympus CKX53, Olympus Corporation, Japan), and photographs of the whole plate were taken.

Wound Healing Assay

Suspensions of 231 and 468 cells were seeded into 6-well plates. The tips of 1-mL blue pipette tips were used to scratch 90% confluent cell monolayers. KLTi was subsequently added at different concentrations for further incubation. Images were recorded under a microscope (Olympus CKX53, Olympus Corporation, Japan) at 0, 24 and 48 h after scratching. Wound closure was measured using ImageJ software.

Cell Apoptosis Assay

Cell apoptosis was detected using an Annexin V-FITC Apoptosis Detection Kit (Beyotime, China). Briefly, 231 and 468 cell suspensions were seeded into 6-well plates and preincubated for 24 h. The cells were then treated with different doses of KLTi and incubated for another 48 h at 37°C. Then, a 20-minute incubation with annexin V-FITC and propidium iodide was performed on the cells. Apoptosis was assessed by flow cytometry (CytoFlex; Beckman Coulter, USA).

Cell Cycle Analysis

Cell cycle analysis was performed using a Cell Cycle and Apoptosis Analysis Kit (Beyotime, China). Cells were collected after treatment with different concentrations of KLTi and fixed with 70% ethanol at 4°C for 24 h. Cell samples

were then stained with propidium iodide staining solution and incubated in the dark for 30 minutes at 37°C. The cell cycle was detected by flow cytometry. The proportions of each phase cells were calculated by Modfit software (version 5.0; Verity Software House, USA).

Quantitative Real-Time Polymerase Chain Reaction (RT-PCR)

Total RNA was extracted from TNBC cells using the TRIzol reagent (Beyotime, China). cDNA was obtained using premixed reverse transcription reagents. An RT-PCR system (CFX96; Bio-Rad, Hercules, USA) was used to amplify cDNA to compare gene expression between groups. All reactions were performed in triplicate. The sequences of the primers used are listed in Table 1.

Western Blot

Cellular protein samples were extracted using RIPA lysis buffer. After quantification with the BCA Protein Assay Kit (Beyotime, China), the concentration of each sample was adjusted. Samples were mixed with SDS-PAGE protein loading buffer and stored at −20°C. The mixed samples were electrophoresed with 120V for 1h and transferred to a 0.45-um poly vinylidene fluoride membrane. Then, the membrane was blocked and incubated with primary antibody for 12h (4°C), followed by secondary antibody incubation for 1h and detection (ChemiDoc MP; Bio-Rad, USA). The antibodies used in this study were β-actin rabbit monoclonal antibody (AF5003, Beyotime, China), CDK1 rabbit polyclonal antibody (AF0111, Beyotime, China), Phospho-CDK1 (pCDK1, Tyr15) rabbit polyclonal antibody (AF5761, Beyotime, China), and HRP-labeled goat anti-rabbit IgG (H+L) (A0208, Beyotime, China).

Statistical Analysis

Statistical analyses were performed using the GraphPad Prism (version 8.0; GraphPad Software, USA) software. All quantitative data were obtained from three different samples, representing at three independent experiments, and presented as mean ± standard deviation (SD). The data distribution was evaluated using Shapiro–Wilk test and QQ plot. The results conforming to normal distribution were analyzed using *t*-tests or one-way ANOVA tests followed by Dunnett's multiple comparison test. The values of $p < 0.05$ (*) or $p < 0.01$ (**) represented significant difference and very significant difference, respectively.

Results

Active Compounds and Potential Targets of KLTi

A total of 38 compounds of KLTi were screened based on previous publications and the TCMSP database. Candidate compounds with DL ≥0.18 were included in the study (18 active ingredients). Among them, four active compounds had DL >0.18, but their molecular formula was not clear. Finally, the information of the 14 compounds was inputted into the Swiss Target Prediction database, DrugBank and TargetNet to obtain the predicted targets. The general information,

Table 1 The Sequences of the Gene Primers

Gene	Forward	Reverse
CDK1	AAACTACAGGTCAAGTGGTAGCC	TCCTGCATAAGCACATCCTGA
CDK2	CCAGGAGTTACTTCTATGCCTGA	TTCATCCAGGGGAGGTACAAC
CHEK1	ATATGAAGCGTGCCGTAGACT	TGCCTATGTCTGGCTCTATTCTG
CDC25A	GTGAAGGCGCTATTTGGCG	TGGTTGCTCATAATCACTGCC
CDC25B	ACGCACCTATCCCTGTCTC	CTGGAAGCGTCTGATGGCAA
MELK	TCTCCCAGTAGCATTCTGCTT	TGATCCAGGGATGGTTCAATAGA
AURKA	GAGGTCCAAAACGTGTTCTCG	ACAGGATGAGGTACACTGGTTG
GAPDH	GGAGTGAGTGGAAGACAGAATGGAAG	CCTACAGCAGAGAAGCAGACAGTTATG

Abbreviations: CDK1, cyclin-dependent kinase 1; CDK2, cyclin-dependent kinase 2; CHEK1, checkpoint kinase 1; CDC25A, cell division cycle 25A; CDC25B, cell division cycle 25B; MELK, maternal embryonic leucine zipper kinase; AURKA, aurora kinase A.

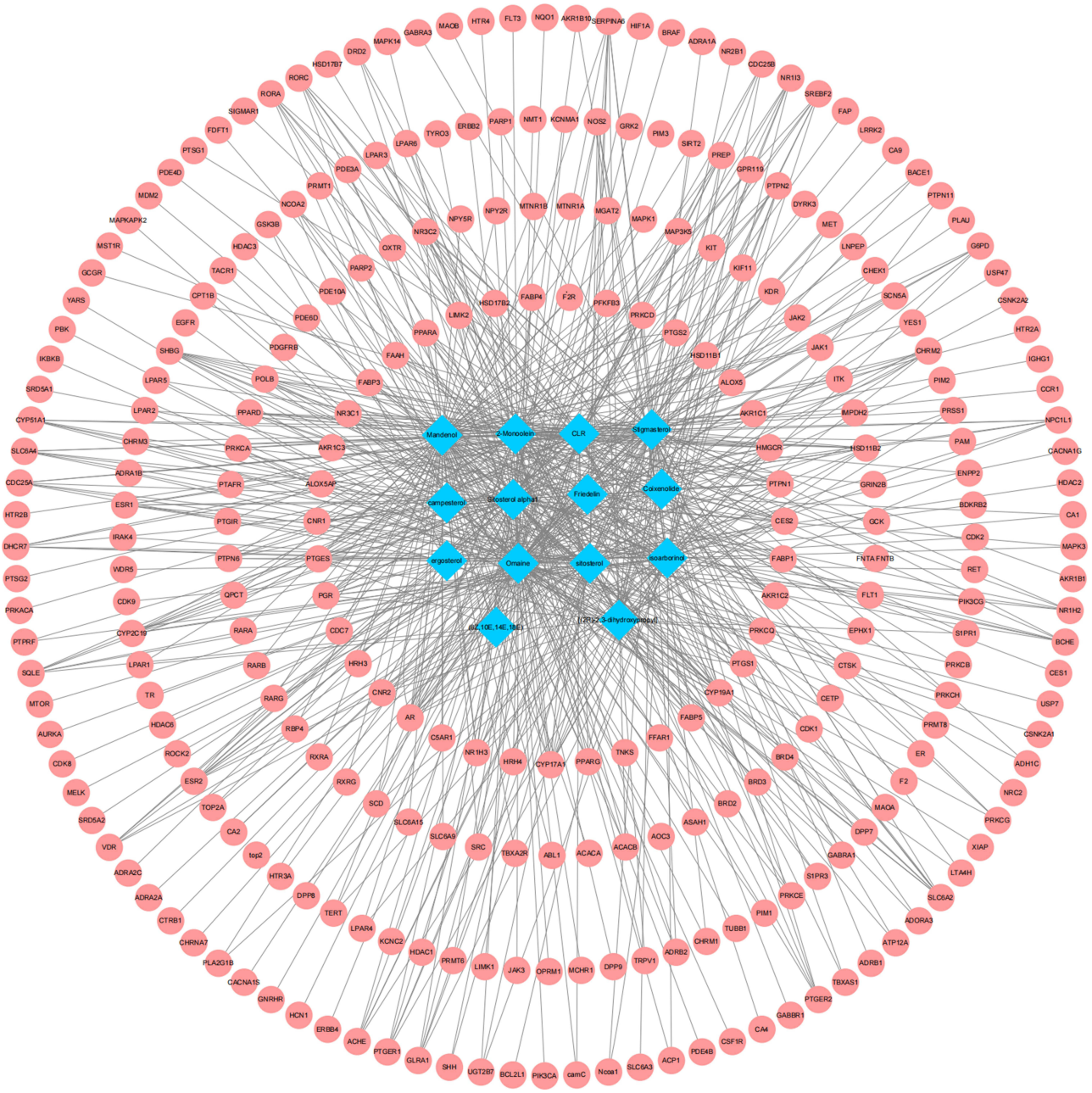

Figure 2 The compound-target network diagram of Kanglaite injection.
Abbreviations: (6Z,10E,14E,18E), (6Z,10E,14E,18E)-2,6,10,15,19,23-hexamethyltetracosa-2,6,10,14,18,22-hexaene; [(2R)-2,3-dihydroxypropyl], [(2R)-2,3-dihydroxypropyl] (Z)-octadec-9-enoate.

including molecule name, molecular formula, and SMILES information of the 14 compounds is shown in Supplementary Table S1, and the compound-target network diagram of the 14 compounds and 281 predicted targets is shown in Figure 2. There were 295 nodes (14 compounds and 281 targets) and 691 edges in the network, representing the relationship between compounds and targets.

TNBC-Related Targets

The GSE38959 in the GEO database, including total RNA expression data which was analyzed with "Agilent-014850 Whole Human Genome Microarray 4x44K G4112F" from 30 TNBC tumor tissues and 13 normal mammary gland ductal tissues, was selected to identify related targets. A total of 3593 DEGs, including 2469 upregulated genes and 1124

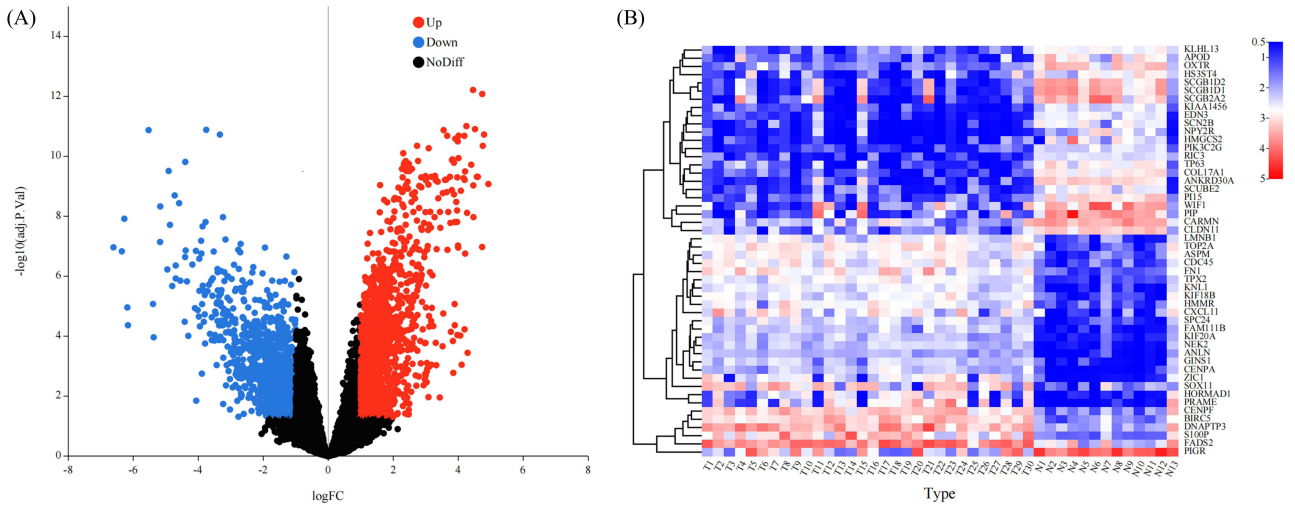

Figure 3 The DEGs in TNBC. (**A**) The volcano map of DEGs in TNBC; (**B**) the heat map of DEGs in TNBC.
Abbreviations: T, tumor tissue; N, normal tissue; DEGs, differentially expressed genes; TNBC, triple-negative breast cancer.

downregulated genes, were screened under the conditions of |log2FC|>1 and adjusted p-value <0.05. The volcano and heat maps are shown in Figure 3A and B, respectively.

Candidate Targets for KLTi Treatment of TNBC

The DEGs and target genes of KLTi were merged using Venny 2.1.0, and 53 overlapping genes were considered candidate targets, as shown in Figure 4A. Based on these genes, a compound-target network was constructed (Figure 4B), the nodes represented compounds or targets, and edges represented interaction relationships. The network contains 67 nodes (14 compounds and 53 targets) and 133 edges. The top four key active compounds in KLTI were isoarborinol, sitosterol alpha1, omaine and mandenol, with the highest degree values of 20, 20, 17, and 16, respectively.

PPI Network Construction and Analysis

The 53 overlapping genes were subjected to STRING to obtain the PPI data. A network was constructed and visualized using Cytoscape. As shown in Figure 4C, the PPI network comprised 45 nodes and 169 edges. A higher degree indicates a larger node size; red indicates the highest degree, and pink indicates the lowest degree. The top three nodes based on

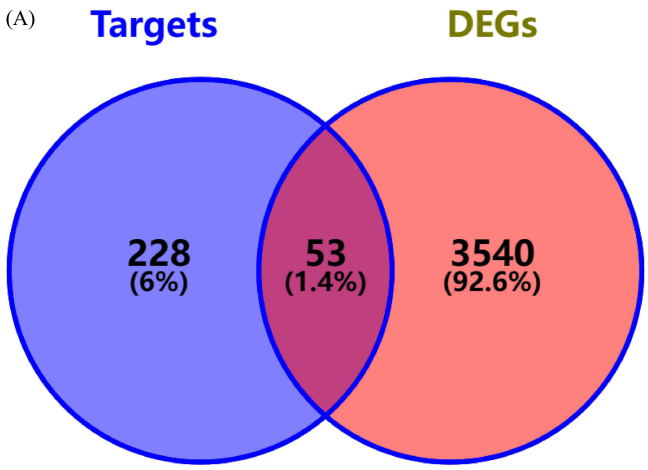

Figure 4 Continued.

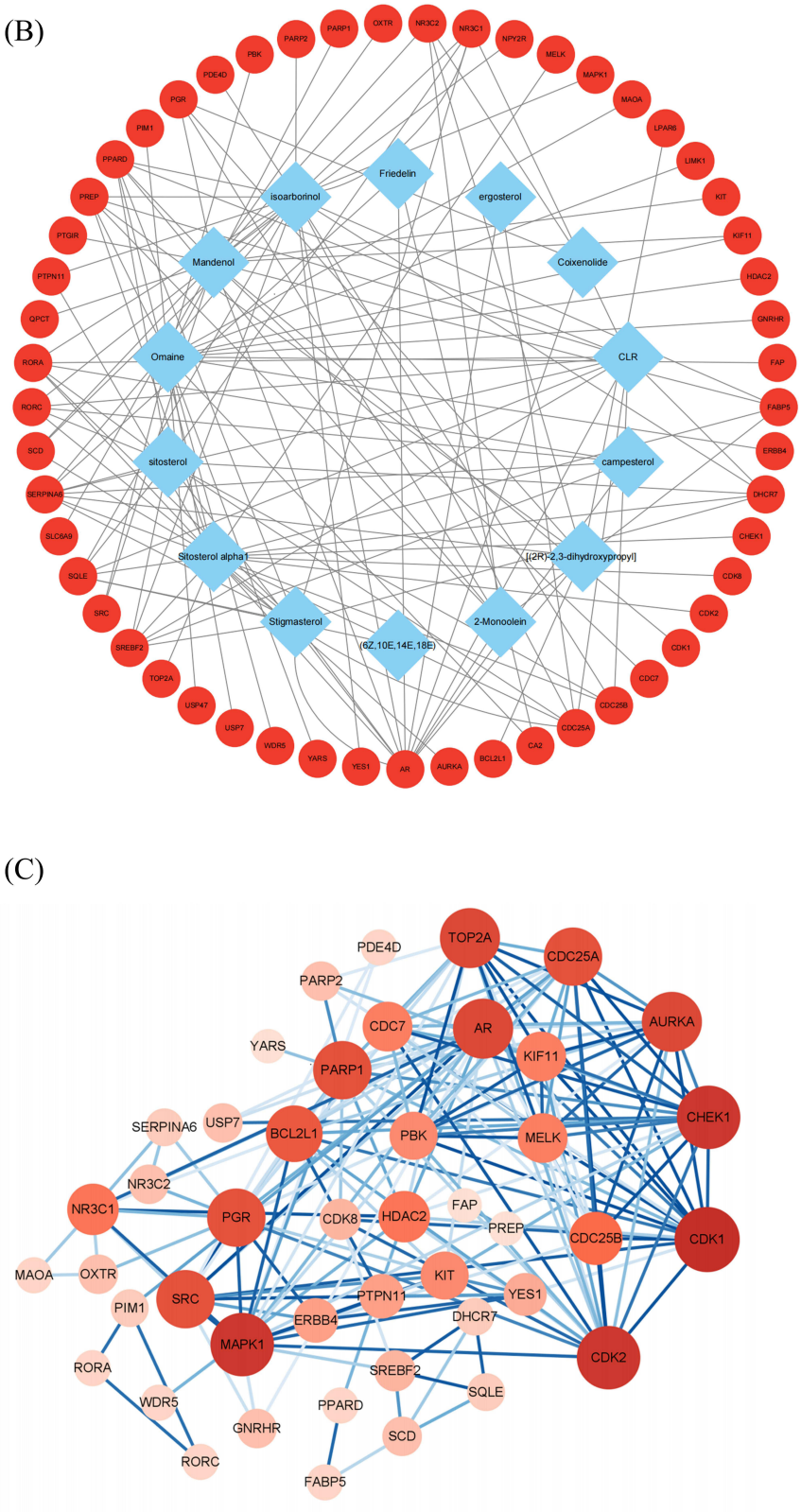

Figure 4 The candidate targets for Kanglaite injection treatment of TNBC. (**A**) Venn diagram of compound targets and DEGs; (**B**) compound-target network of Kanglaite injection against TNBC; (**C**) PPI network diagram of candidate genes.

Abbreviations: TNBC, triple-negative breast cancer; DEGs, differentially expressed genes; (6Z,10E,14E,18E), (6Z,10E,14E,18E)-2,6,10,15,19,23-hexamethyltetracosa-2,6,10,14,18,22-hexaene; [(2R)-2,3-dihydroxypropyl], [(2R)-2,3-dihydroxypropyl] (Z)-octadec-9-enoate; PPI, protein–protein interaction.

degree values were cyclin-dependent kinase 1 (CDK1), cyclin-dependent kinase 2 (CDK2), and checkpoint kinase 1 (CHEK1), which may play a key role in the PPI network against TNBC.

Potential Pathways of KLTi

Fifty-three overlapping genes were entered into the Metascape system for the GO and KEGG pathway analyses. GO analysis revealed targets related to biological processes, cellular components, and molecular functions associated with KLTi treatment. Based on p-values <0.05, 365 enriched biological processes were identified, of which the first five were protein phosphorylation, intracellular receptor signaling pathway, G2/M transition of mitotic cell cycle, cell cycle G2/M phase transition, and regulation of G2/M transition of mitotic cell cycle (Figure 5A). The targets and rankings of cell components and molecular functions are shown in Figure 5B and C, respectively. In addition, we performed KEGG pathway analysis and identified 56 pathways based on p-value <0.05, including pathways in cancer, cell cycle, progesterone-mediated oocyte maturation, viral carcinogenesis and oocyte meiosis (Figure 5D).

Molecular Docking and Analysis

Based on the PPI network and the results of the pathway enrichment analyses, the top three targets, CDK1, CDK2, and CHEK1 were selected for molecular docking. The binding energies of the KLTi components with the targets are shown in Table 2 and Supplementary Table S2. It is generally believed that the binding capacity is stronger when the binding energy is lower than −5 kcal/mol. Eight of the 14 KLTi compounds had binding energies less than −5 kcal/mol to CDK1,

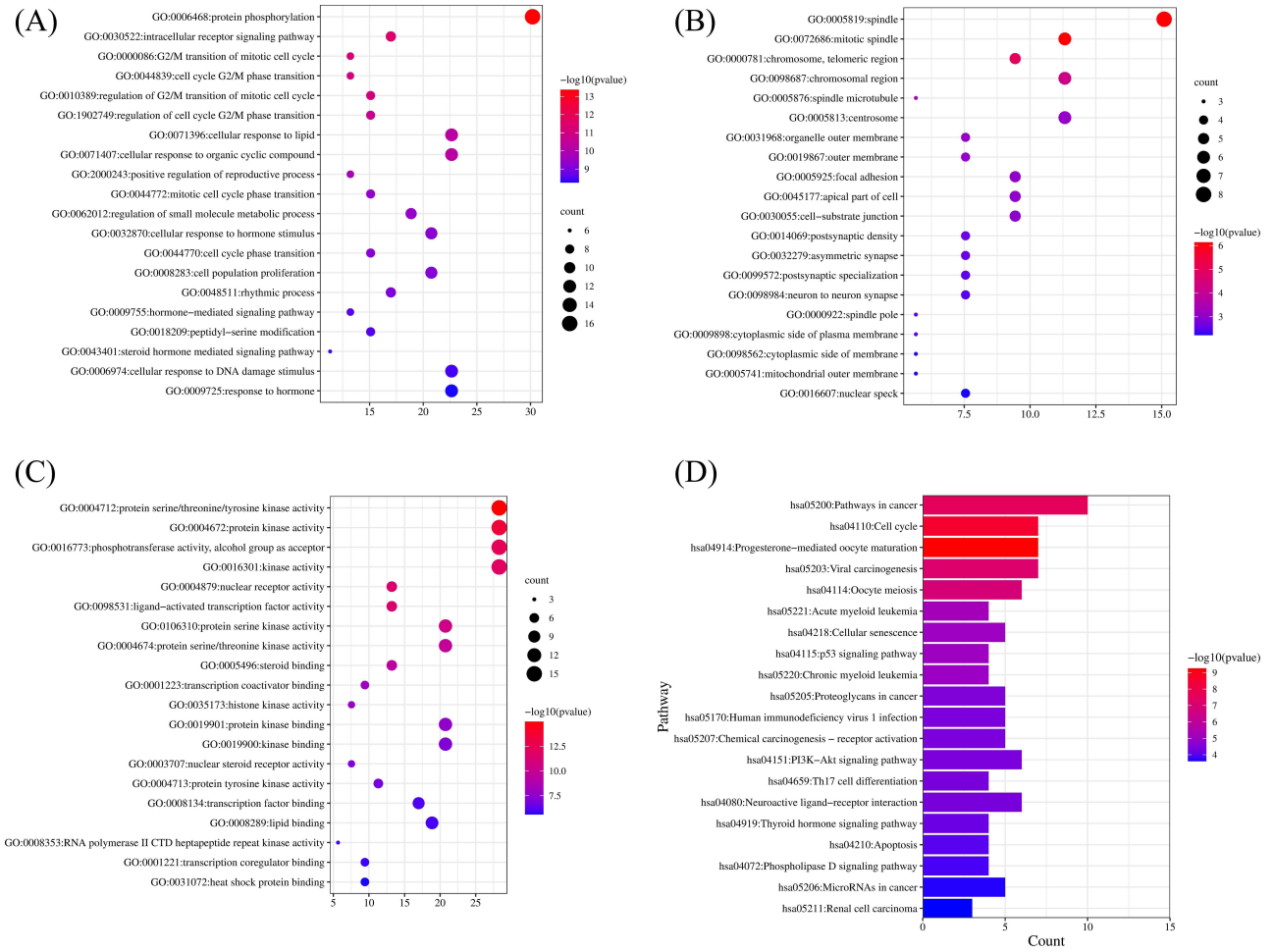

Figure 5 The potential pathways of Kanglaite injection. (**A**) GO biological processes; (**B**) GO cell components; (**C**) GO molecular functions; (**D**) KEGG pathway of KLTi. **Abbreviations**: GO, Gene Ontology Consortium; KEGG, Kyoto Encyclopedia of Genes and Genomes.

Table 2 The Binding Energy of the Main Active Compounds to the Targets

Target / Active Compound	CDK1 (PDB ID:6GU2) (kcal/mol)	CDK2 (PDB ID:7VDU) (kcal/mol)	CHEK1 (PDB ID:2YEX) (kcal/mol)
Isoarborinol	−6.99	−8.27	−6.56
Sitosterol alpha1	−6.45	−9.18	−6.67

Abbreviations: CDK1, cyclin-dependent kinase 1; CDK2, cyclin-dependent kinase 2; CHEK1, checkpoint kinase 1.

CDK2, and CHEK1, which implies that these compounds have good affinity to the targets. The docking results of sitosterol alpha1 and isoarborinol, the two active ingredients with the highest drug-like properties and the highest degree values, with the three main targets CDK1, CDK2 and CHEK1 are shown in Figure 6 and Supplementary Table S3. The pink structures represent the compound ligands, blue-green-red structures represent the residues attached to the ligand on the target protein, and the yellow dashed lines represent attached hydrogen bond.

KLTi Suppresses TNBC Cell Proliferation and Migration

CCK-8 assays were performed to determine the anticancer effects of different concentrations of KLTi on 231 and 468 cells for 48 and 72 h. As shown in Figure 7A, KLTi significantly decreased the viability of 231 and 468 cells in time- and dose-dependent manner. The IC50 values of KLTi in 231 cells were 547.1 ug/mL and 304.9 ug/mL, and 553.9 ug/mL and 323.7 ug/mL in 468 cells for 48 and 72 h, respectively. Subsequently, concentrations of 0, 250 and 500 ug/mL were selected for further studies. The results of colony formation assays showed that the number of cell colonies decreased with increasing KLTi concentration, as shown in Figure 7B, which also indicated that KLTi could inhibit TNBC cell proliferation. In addition, KLTi significantly inhibited TNBC cell migration (Figure 7C).

KLTi Induces Apoptosis and Cell Cycle Arrest

After 48 h of incubation, the apoptosis of 231 and 468 cells significantly increased with increasing KLTi concentrations, as shown in Figure 8A. Cell cycle analysis indicated that KLTi treatment induced G2/M phase arrest in 231 and 468 cells (Figure 8B).

Cell Cycle Arrest Mechanism Plays an Important Role in the Inhibition of KLTi on TNBC

Cell cycle genes were identified by GO-BP analysis and validated in vitro by RT-PCR as shown in Figure 9. The mRNA expression of CDK1, CDK2, CHEK1, cell division cycle 25A (CDC25A), cell division cycle 25B (CDC25B),

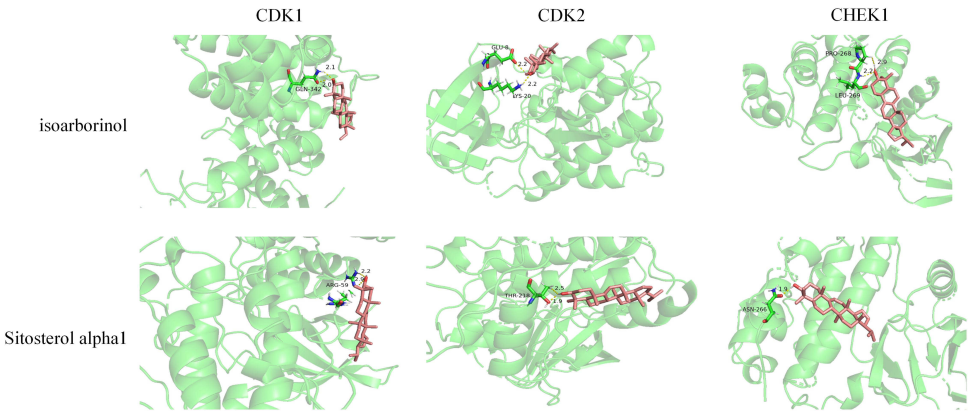

Figure 6 Molecular docking of compounds with targets.
Abbreviations: CDK1, cyclin-dependent kinase 1; CDK2, cyclin-dependent kinase 2; CHEK1, checkpoint kinase 1.

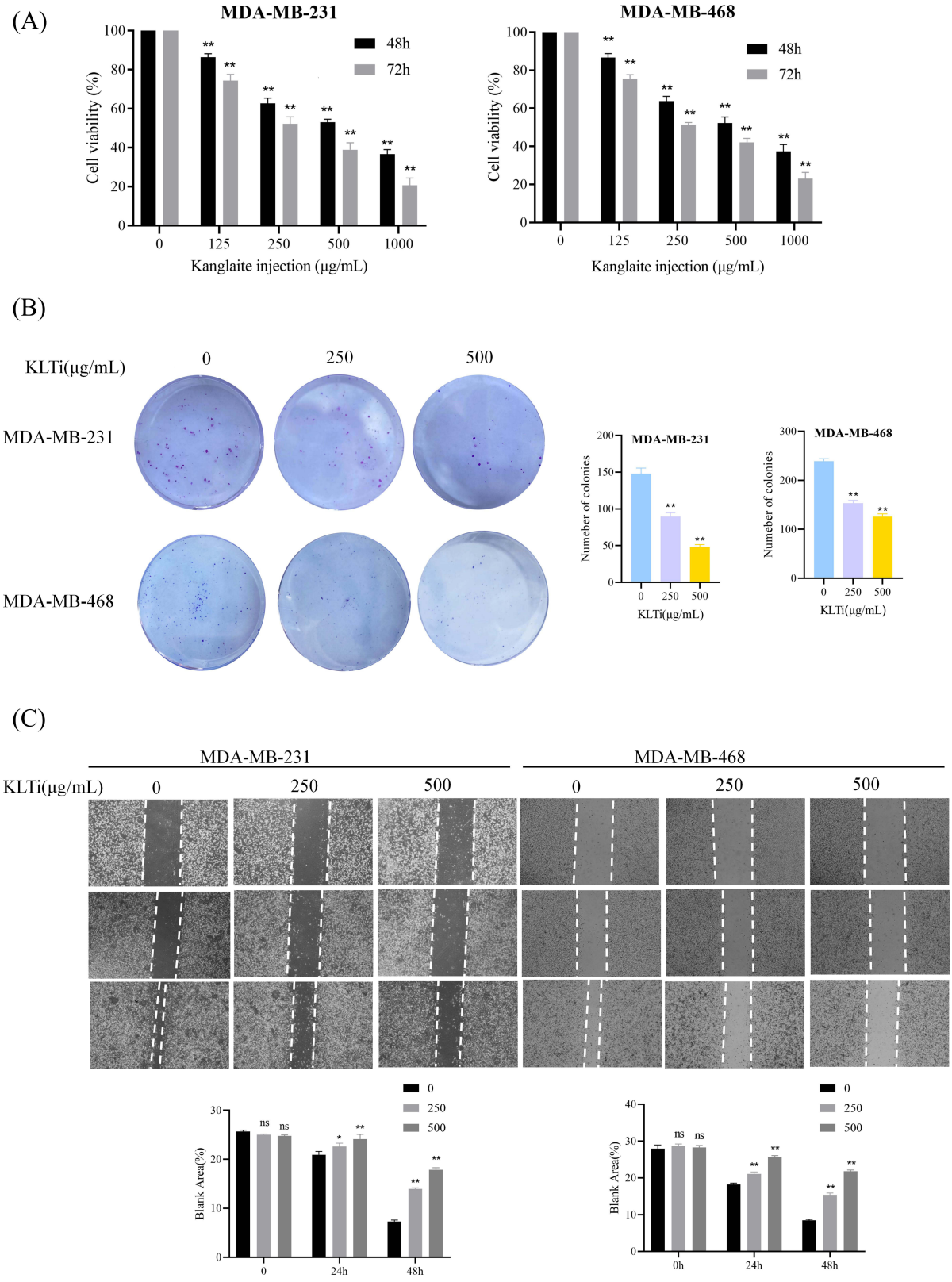

Figure 7 Kanglaite injection inhibits the growth of TNBC cells in vitro. (**A**) KLTi shows a dose- and time-dependent effect on the viability of TNBC cells; (**B**) KLTi shows a dose-reduced colony formation in TNBC cells; (**C**) KLTi shows the ability to inhibit the migration of TNBC cells. (ns, not significant *p < 0.05, **p < 0.01, vs 0 Group). **Abbreviations**: KLTi, Kanglaite injection; TNBC, triple-negative breast cancer; ns, no significance.

https://doi.org/10.2147/DDDT.S397969 DovePress

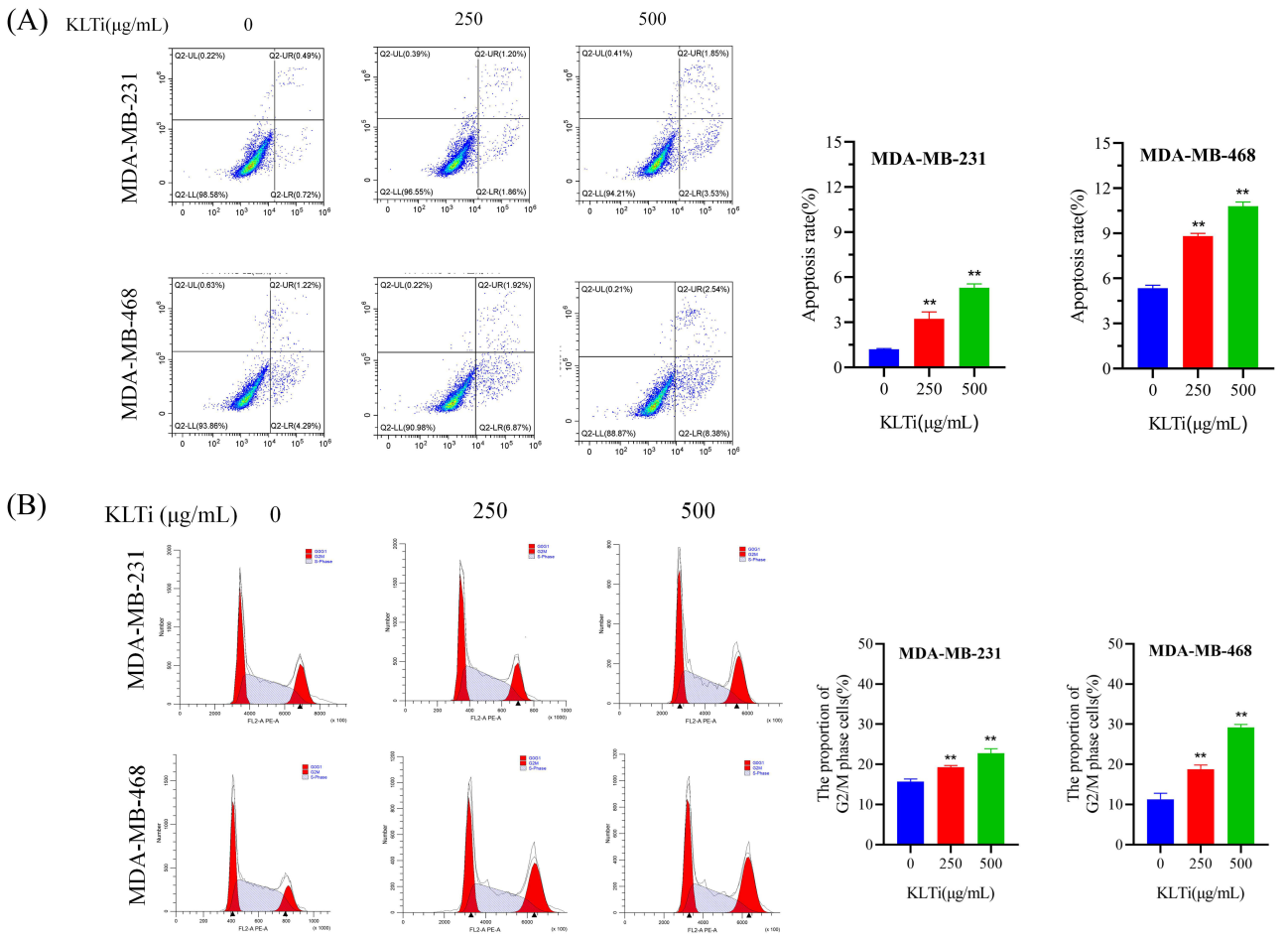

Figure 8 Kanglaite injection induces apoptosis and arrests the cell cycle at the G2/M phase in TNBC cells. (**A**) KLTi induced MDA-MB-231 and MDA-MB-468 cells apoptosis; (**B**) KLTi arrested MDA-MB-231 and MDA-MB-468 cells in the G2/M phase. (**p < 0.01 vs 0 Group).
Abbreviations: KLTi, Kanglaite injection; TNBC, triple-negative breast cancer.

maternal embryonic leucine zipper kinase (MELK), and aurora kinase A (AURKA) (G2/M phase-related genes by GO BP and KEGG analysis) were down-regulated in cancer cells after the treatment with KLTi. Western blot was used to detect the levels of CDK1 and pCDK1, which are proteins known to play important roles in cell cycle progression. The results showed that KLTi downregulated the expression of CDK1 and upregulated the expression of pCDK1 (Figure 10).

Discussion

The advent of the big data era and the development of bioinformatics methods have provided tremendous assistance in the discovery of antitumor drugs through network pharmacology.[29] The core principle of network pharmacology is to examine the biological pathways of medicinal compounds from a network perspective to predict the desired targets.[30,31] In this study, a network pharmacology approach, molecular docking and in vitro experimental validation were utilized to reveal the bioactive compounds and molecular mechanisms of KLTi in the treatment of TNBC. A total of 14 active compounds, 281 KLTi targets, and 3593 therapeutic targets for TNBC were selected from public databases, and 53 candidate targets of KLTi for TNBC treatment were identified by searching for intersections between targets. The compound-target network demonstrated that isoarborinol and sitosterol alpha1 were the two most active compounds. The PPI network showed the interaction of the proteins, suggesting that CDK1, CDK2, and CHEK1 may play a key role in the action of KLTi on TNBC. GO enrichment analyses annotated the biological functions of targets in three aspects: BP, CC and MF. KEGG pathway analysis identified 56 pathways based on p-value <0.05, and the most important cancer-

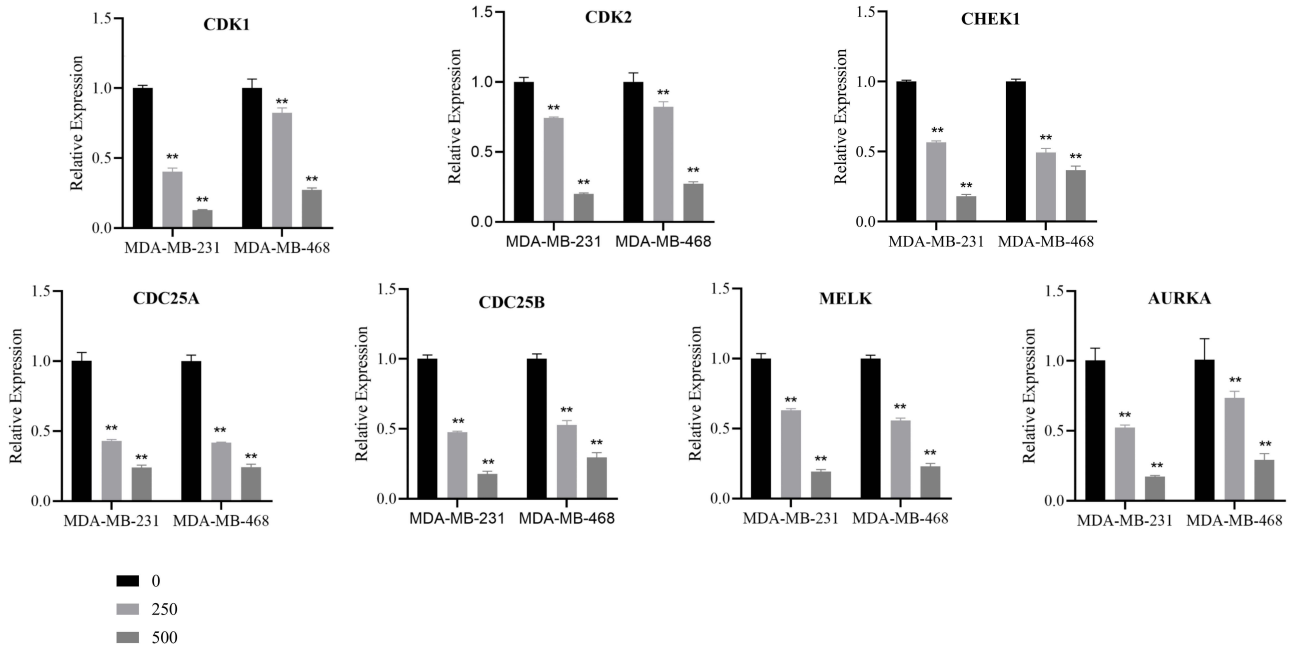

Figure 9 The mRNA expression of G2/M-related genes after treatment with Kanglaite injection. The mRNA expressions of CDK1, CDK2, CHEK1, CDC25A, CDC25B, MELK and AURKA are downregulated in MDA-MB-231 and MDA-MB-468 cells after treatment with Kanglaite injection. (**p < 0.01 vs 0 Group).
Abbreviations: CDK1, cyclin-dependent kinase 1; CDK2, cyclin-dependent kinase 2; CHEK1, checkpoint kinase 1; CDC25A, cell division cycle 25A; CDC25B, cell division cycle 25B; MELK, maternal embryonic leucine zipper kinase; AURKA, aurora kinase A.

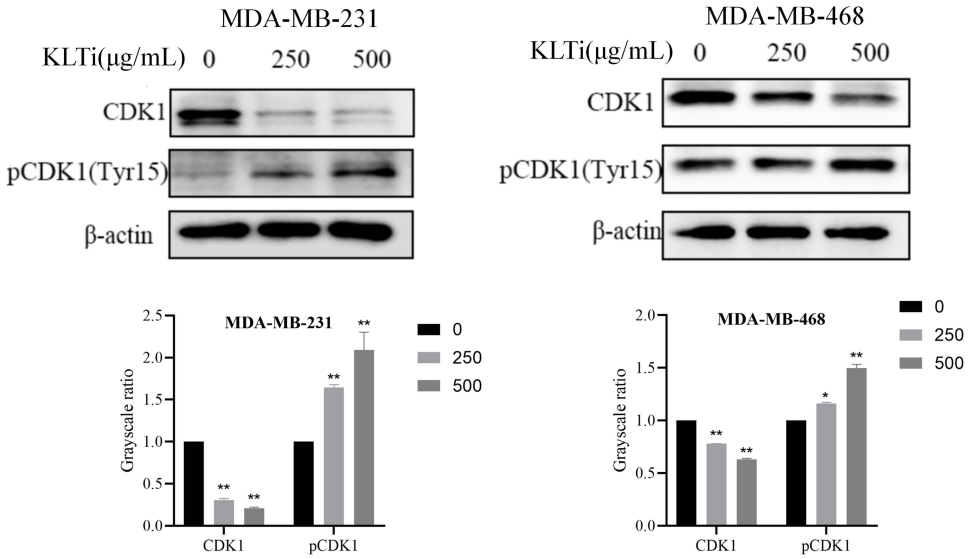

Figure 10 Protein expression in MDA-MB-231 and MDA-MB-468 cells after Kanglaite injection intervention. Kanglaite injection upregulates pCDK1 (Tyr15) and downregulates CDK1 expression. (*p < 0.05, **p < 0.01 vs 0 Group).
Abbreviations: CDK1, cell cycle protein-dependent kinase 1; pCDK1, phospho-cell cycle protein-dependent kinase 1.

related pathway was cell cycle. Molecular docking results showed that the important compounds combined well to the target proteins. The results of cell experiments confirmed that KLTi blocks cell cycle progression and induces apoptosis of TNBC cells by downregulating the expression of cell cycle-related genes (CDK1, CDK2, CHEK1, CDC25A, CDC25B, MELK, and AURKA) and preventing the activation of CDK1 dephosphorylation.

TNBC has the worst prognosis of all BC subtypes, with a recurrence rate of more than 50% in the first 3–5 years after diagnosis and a median survival of approximately 10.2 months.[32,33] Due to the lack of relevant receptor markers, patients

cannot benefit from endocrine or HER2-targeting drugs. Less than 30% of TNBC patients achieve a complete response with standard chemotherapy regimens, such as taxanes or anthracyclines.[3] Therefore, therapeutic agents for TNBC have become a popular research topic. KLTi is mainly composed of Coix seed extract. This seed has been reported to have anti-allergic, anti-inflammatory, antioxidant, hypolipidemic, and anti-tumor effects.[34–37] Clinical application of KLTi in the treatment of BC has revealed that patients who receive combined chemotherapy demonstrated improved levels of T cell subsets, quality of life, and enhanced immune function.[10,11] However, there are currently no clinical data on KLTi in TNBC patients. A preclinical study found that KLTi can inhibit tumor growth in a TNBC mouse model, exerting an anti-TNBC effect by interfering with the miR-205/S1PR1 axis, regulating sphingomyelin metabolism, and partially affecting the downstream STAT3/MAPK/AKT signaling pathway.[13] The active compound sitosterol alpha1 is converted from sterols. Sterols are essential in eukaryotes and participate in cell membrane function and signal transduction.[38–40] However, its significance in specific diseases has not yet been revealed, and further research is pending. Isoarborinol, another active compound, was first isolated from higher plants in the 1960s, and research on its function remains non-existent.[41] Both this study and previous studies have selected it as the anticancer active compound of KLTi. We believe that isoarborinol is worthy of further study.

The PPI results suggested that CDK1, CDK2 and CHEK1, especially CDK1, may play a key role in the anti-TNBC process. KEGG analysis showed that cancer pathways and cell cycle signaling pathways exhibit the highest number of genes enriched in tumor-associated signaling pathways and play a key role in the action of KLTi on TNBC. Molecular docking results showed that the main active compounds of KLTi were able to successfully dock with CDK1, CDK2, and CHEK1 with strong affinity. The CCK-8 assay, colony formation assay, wound healing assay, and cell apoptosis assay were performed to demonstrate that KLTi inhibited TNBC cell line proliferation, migration, and induced apoptosis. Cell cycle analysis, RT-PCR, and Western blot were performed to reveal that KLTi caused TNBC cell lines to be arrested in G2/M phase by affecting the expression of CDK1, CDK2, CHEK1, CDC25A, CDC25B, MELK, and AURKA genes. These results suggested that KLTi exerts therapeutic effects on TNBC by affecting cell cycle.

Cell cycle therapy for tumors has received considerable attention in recent years. Under physiological conditions, the normal cell cycle is regulated by several factors such as cell cycle protein-dependent kinase (CDK), cell cycle proteins, and CDK inhibitors.[42,43] Aberrant activity of the core cell cycle machinery is seen in essentially all tumor types and is a driver of tumorigenesis, as well as in TNBC.[44,45] CDK1 and related molecules play a major role in the cell cycle, and CDK1 expression is upregulated in many human cancers.[46–48] The CDK1-cyclin B1 complex (M-phase promoter) is necessary for transitioning from S to G2/M in the cell cycle.[49] By phosphorylation of the Thr161 amino acid activation site and dephosphorylation of the Thr14/Tyr15 amino acid inhibition site, CDK1 is activated. In the G2 phase, Wee1 kinase phosphorylates Thr14 and Tyr15 of CDK1 to inactivate it, allowing the continuous accumulation of CDK-cyclinB1. In the M phase, decreased Wee1 activity and CDC25 contribute to CDK dephosphorylation and CDK1 activation.[49,50] This process is aberrantly enhanced in malignant tumors. In this study, we demonstrated by RT-PCR that the expression of G2/M-related genes, including CDK2, CHEK1, CDC25A, CDC25B, MELK, and AURKA, which play roles in dephosphorylation or phosphorylation of CDK1, were downregulated in TNBC cell lines after KLTi intervention. Western blot analysis showed that the expression of pCDK1 (Tyr15) was increased, and the expression of CDK1 was decreased. In the presence of reduced total protein CDK1 expression, pCDK1 expression was still increased, probably because the pCDK1 dephosphorylation process was disturbed. These findings suggest that KLTi may affect the dephosphorylation and activation of CDK1 in the G2/M phase, thereby blocking 231 and 468 cells in the G2/M phase, inhibiting proliferation, and inducing apoptosis in TNBC cells, which warrants further investigation.

The small sample size is one of the limitations of this study. Secondly, cell cycle target proteins were not knocked out or overexpressed to determine whether they were important targets of KLTi. Thirdly, there is a lack of animal experiments to demonstrate the anti-TNBC effects of KLTi in vivo. Fourthly, the upstream and downstream targets of CDK1, such as Wee1 and CDC25, and their interactions with CDK1 should be further investigated. Last but not least, well-designed RCTs can help to provide key clinical information and provide a stronger rationale for the clinical use of KLTi in the treatment of TNBC. Therefore, more experiments are needed to further explore the role of KLTi in TNBC treatment and clarify its mechanism.

Conclusions

In this study, network pharmacology, molecular docking technology and in vitro experiments were performed to prove that KLTi can prevent cell cycle progression by inhibiting cell cycle gene expression and CDK1 dephosphorylation activation, thus achieving an anti-TNBC effect.

Abbreviations

BC, breast cancer; TNBC, triple-negative breast cancer; KLTi, Kanglaite injection; TCM, traditional Chinese medicine; TCMSP, Traditional Chinese Medicine Database and Analysis Platform; ADME, absorption, distribution, metabolism and excretion; OB, oral bioavailability; DL, drug-likeness; SMILES, simplified molecular input line entry specification; DEGs, differentially expressed genes; PPI, protein–protein interaction; GO, Gene Ontology Consortium; KEGG, Kyoto Encyclopedia of Genes and Genomes; BP, biological processes; MF, molecular functions; CC, cellular component; PDB, Protein Data Bank; 231, MDA-MB-231; 468, MDA-MB-468; CCK-8, Cell Counting Kit-8; RT-PCR, Quantitative Real-Time Polymerase Chain Reaction; WB, Western Blot; SD, standard deviation; CDK1, cyclin-dependent kinase 1; CDK2, cyclin-dependent kinase 2; CHEK1, checkpoint kinase 1; CDC25A, cell division cycle 25A; CDC25B, cell division cycle 25B; MELK, maternal embryonic leucine zipper kinase; AURKA, aurora kinase A.

Acknowledgement

The authors would like to acknowledge Professor, Yanfeng Zou, for advice on data statistics.

Disclosure

The authors declare that there are no conflicts of interest.

References

1. Sung H, Ferlay J, Siegel RL, et al. Global cancer statistics 2020: GLOBOCAN estimates of incidence and mortality worldwide for 36 cancers in 185 countries. *CA Cancer J Clin*. 2021;71(3):209–249. doi:10.3322/caac.21660
2. Bray F, Ferlay J, Soerjomataram I, Siegel RL, Torre LA, Jemal A. Global cancer statistics 2018: GLOBOCAN estimates of incidence and mortality worldwide for 36 cancers in 185 countries. *CA Cancer J Clin*. 2018;68(6):394–424. doi:10.3322/caac.21492
3. Li Y, Zhang H, Merkher Y, et al. Recent advances in therapeutic strategies for triple-negative breast cancer. *J Hematol Oncol*. 2022;15(1):121. doi:10.1186/s13045-022-01341-0
4. Dent R, Trudeau M, Pritchard KI, et al. Triple-negative breast cancer: clinical features and patterns of recurrence. *Clin Cancer Res*. 2007;13 (15 Pt 1):4429–4434. doi:10.1158/1078-0432.CCR-06-3045
5. Carey LA, Dees EC, Sawyer L, et al. The triple negative paradox: primary tumor chemosensitivity of breast cancer subtypes. *Clin Cancer Res*. 2007;13(8):2329–2334. doi:10.1158/1078-0432.CCR-06-1109
6. Asleh K, Riaz N, Nielsen TO. Heterogeneity of triple negative breast cancer: current advances in subtyping and treatment implications. *J Exp Clin Cancer Res*. 2022;41(1):265. doi:10.1186/s13046-022-02476-1
7. Liu X, Xu F, Wang G, Diao X, Li Y. Kanglaite injection plus chemotherapy versus chemotherapy alone for non-small cell lung cancer patients: a systematic review and meta-analysis. *Curr Ther Res Clin Exp*. 2008;69(5):381–411. doi:10.1016/j.curtheres.2008.10.004
8. Zhan YP, Huang XE, Cao J, et al. Clinical safety and efficacy of Kanglaite® (Coix Seed Oil) injection combined with chemotherapy in treating patients with gastric cancer. *Asian Pac J Cancer Prev*. 2012;13(10):5319–5321. doi:10.7314/apjcp.2012.13.10.5319
9. Schwartzberg LS, Arena FP, Bienvenu BJ, et al. A randomized, open-label, safety and exploratory efficacy study of Kanglaite Injection (KLTi) plus gemcitabine versus gemcitabine in patients with advanced pancreatic cancer. *J Cancer*. 2017;8(10):1872–1883. doi:10.7150/jca.15407
10. Guo HY, Cai Y, Yang XM, et al. Randomized Phase II trial on mitomycin-C/cisplatin ± KLT in heavily pretreated advanced breast cancer. *Am J Chin Med*. 2008;36(4):665–674. doi:10.1142/S0192415X08006132
11. Cheng S, Qu B, Qiu X, Li N, Wang X, Hao J. Efficacy and safety of Kanglaite injection combined with chemotherapy for women breast cancer. *Medicine*. 2021;100(22):e26245. doi:10.1097/MD.0000000000026245
12. Liu Y, Zhang W, Wang XJ, Liu S. Antitumor effect of Kanglaite® injection in human pancreatic cancer xenografts. *BMC Complement Altern Med*. 2014;14:228. doi:10.1186/1472-6882-14-228
13. Fang T, Jiang YX, Chen L, et al. Coix seed oil exerts an anti-triple-negative breast cancer effect by disrupting miR-205/S1PR1 axis. *Front Pharmacol*. 2020;11:529962. doi:10.3389/fphar.2020.529962
14. Li S, Zhang B. Traditional Chinese medicine network pharmacology: theory, methodology and application. *Chin J Nat Med*. 2013;11(2):110–120. doi:10.1016/S1875-5364(13)60037-0
15. Zeng L, Yang K. Exploring the pharmacological mechanism of Yanghe Decoction on HER2-positive breast cancer by a network pharmacology approach. *J Ethnopharmacol*. 2017;199:68–85. doi:10.1016/j.jep.2017.01.045
16. Zheng J, Wu M, Wang H, et al. Network pharmacology to unveil the biological basis of health-strengthening herbal medicine in cancer treatment. *Cancers*. 2018;10(11):E461. doi:10.3390/cancers10110461

17. Xu B, Dan W, Zhang X, et al. Gene differential expression and interaction networks illustrate the biomarkers and molecular biological mechanisms of unsaponifiable matter in Kanglaite injection for pancreatic ductal adenocarcinoma. *Biomed Res Int*. 2022;2022:6229462. doi:10.1155/2022/6229462
18. Ru J, Li P, Wang J, et al. TCMSP: a database of systems pharmacology for drug discovery from herbal medicines. *J Cheminform*. 2014;6:13. doi:10.1186/1758-2946-6-13
19. Gfeller D, Grosdidier A, Wirth M, Daina A, Michielin O, Zoete V. SwissTargetPrediction: a web server for target prediction of bioactive small molecules. *Nucleic Acids Res*. 2014;42(WebServer issue):W32–38. doi:10.1093/nar/gku293
20. Wishart DS, Feunang YD, Guo AC, et al. DrugBank 5.0: a major update to the DrugBank database for 2018. *Nucleic Acids Res*. 2018;46(D1): D1074–D1082. doi:10.1093/nar/gkx1037
21. Yao ZJ, Dong J, Che YJ, et al. TargetNet: a web service for predicting potential drug–target interaction profiling via multi-target SAR models. *J Comput Aided Mol Des*. 2016;30(5):413–424. doi:10.1007/s10822-016-9915-2
22. Franz M, Lopes CT, Huck G, Dong Y, Sumer O, Bader GD. Cytoscape.js: a graph theory library for visualisation and analysis. *Bioinformatics*. 2016;32(2):309–311. doi:10.1093/bioinformatics/btv557
23. Clough E, Barrett T. The gene expression omnibus database. *Methods Mol Biol*. 2016;1418:93–110. doi:10.1007/978-1-4939-3578-9_5
24. Szklarczyk D, Gable AL, Nastou KC, et al. The STRING database in 2021: customizable protein-protein networks, and functional characterization of user-uploaded gene/measurement sets. *Nucleic Acids Res*. 2021;49(D1):D605–D612. doi:10.1093/nar/gkaa1074
25. Carbon S, Douglass E, Good BM. The gene ontology resource: enriching a gold mine. *Nucleic Acids Res*. 2021;49(D1):1. doi:10.1093/nar/gkaa1113
26. Kanehisa M, Furumichi M, Sato Y, Ishiguro-Watanabe M, Tanabe M. KEGG: integrating viruses and cellular organisms. *Nucleic Acids Res*. 2021;49(D1):D545–D551. doi:10.1093/nar/gkaa970
27. Zhou Y, Zhou B, Pache L, et al. Metascape provides a biologist-oriented resource for the analysis of systems-level datasets. *Nat Commun*. 2019;10 (1):1523. doi:10.1038/s41467-019-09234-6
28. Burley SK, Bhikadiya C, Bi C, et al. RCSB protein data bank: powerful new tools for exploring 3D structures of biological macromolecules for basic and applied research and education in fundamental biology, biomedicine, biotechnology, bioengineering and energy sciences. *Nucleic Acids Res*. 2021;49(D1):D437–D451. doi:10.1093/nar/gkaa1038
29. Hopkins AL. Network pharmacology: the next paradigm in drug discovery. *Nat Chem Biol*. 2008;4(11):682–690. doi:10.1038/nchembio.118
30. Vetrivel P, Murugesan R, Bhosale PB, et al. A network pharmacological approach to reveal the pharmacological targets and its associated biological mechanisms of prunetin-5-o-glucoside against gastric cancer. *Cancers*. 2021;13(8):1918. doi:10.3390/cancers13081918
31. Zhu J, Li B, Ji Y, Zhu L, Zhu Y, Zhao H. β-elemene inhibits the generation of peritoneum effusion in pancreatic cancer via suppression of the HIF1A-VEGFA pathway based on network pharmacology. *Oncol Rep*. 2019;42(6):2561–2571. doi:10.3892/or.2019.7360
32. Bonotto M, Gerratana L, Poletto E, et al. Measures of outcome in metastatic breast cancer: insights from a real-world scenario. *Oncologist*. 2014;19 (6):608–615. doi:10.1634/theoncologist.2014-0002
33. Hallett RM, Dvorkin-Gheva A, Bane A, Hassell JA, Gene A. Signature for predicting outcome in patients with basal-like breast cancer. *Sci Rep*. 2012;2(1):227. doi:10.1038/srep00227
34. Chung CP, Lee MY, Hsia SM, et al. Suppression on allergic airway inflammation of dehulled adlay (Coix lachryma-jobi L. var. ma-yuen Stapf) in mice and anti-degranulation phytosterols from adlay bran. *Food Funct*. 2021;12(24):12788–12799. doi:10.1039/d1fo01621k
35. Bai C, Zheng J, Zhao L, Chen L, Xiong H, McClements DJ. Development of oral delivery systems with enhanced antioxidant and anticancer activity: coix seed oil and β-carotene coloaded liposomes. *J Agric Food Chem*. 2019;67(1):406–414. doi:10.1021/acs.jafc.8b04879
36. Kim SO, Yun SJ, Jung B, et al. Hypolipidemic effects of crude extract of adlay seed (Coix lachrymajobi var. mayuen) in obesity rat fed high fat diet: relations of TNF-alpha and leptin mRNA expressions and serum lipid levels. *Life Sci*. 2004;75(11):1391–1404. doi:10.1016/j.lfs.2004.03.006
37. Zhang W, Jia X, Xu Y, et al. Effects of coix seed extract, bifidobacterium BPL1, and their combination on the glycolipid metabolism in obese mice. *Front Nutr*. 2022;9:939423. doi:10.3389/fnut.2022.939423
38. Yoshida M, Ioki M, Matsuura H, et al. Diverse steroidogenic pathways in the marine alga Aurantiochytrium. *J Appl Phycol*. 2020;32(3):1631–1642. doi:10.1007/s10811-020-02078-4
39. Hannich JT, Umebayashi K, Riezman H. Distribution and functions of sterols and sphingolipids. *Cold Spring Harb Perspect Biol*. 2011;3(5): a004762. doi:10.1101/cshperspect.a004762
40. Desmond E, Gribaldo S. Phylogenomics of sterol synthesis: insights into the origin, evolution, and diversity of a key eukaryotic feature. *Genome Biol Evol*. 2009;1:364–381. doi:10.1093/gbe/evp036
41. Xue Z, Duan L, Liu D, et al. Divergent evolution of oxidosqualene cyclases in plants. *New Phytol*. 2012;193(4):1022–1038. doi:10.1111/j.1469-8137.2011.03997.x
42. Barnum KJ, O'Connell MJ. Cell cycle regulation by checkpoints. *Methods Mol Biol*. 2014;1170:29–40. doi:10.1007/978-1-4939-0888-2_2
43. Lim S, Kaldis P. Cdks, cyclins and CKIs: roles beyond cell cycle regulation. *Development*. 2013;140(15):3079–3093. doi:10.1242/dev.091744
44. Suski JM, Braun M, Strmiska V, Sicinski P. Targeting cell-cycle machinery in cancer. *Cancer Cell*. 2021;39(6):759–778. doi:10.1016/j.ccell.2021.03.010
45. Williams GH, Stoeber K. The cell cycle and cancer. *J Pathol*. 2012;226(2):352–364. doi:10.1002/path.3022
46. Hongo F, Takaha N, Oishi M, et al. CDK1 and CDK2 activity is a strong predictor of renal cell carcinoma recurrence. *Urol Oncol*. 2014;32 (8):1240–1246. doi:10.1016/j.urolonc.2014.05.006
47. Sung WW, Lin YM, Wu PR, et al. High nuclear/cytoplasmic ratio of Cdk1 expression predicts poor prognosis in colorectal cancer patients. *BMC Cancer*. 2014;14:951. doi:10.1186/1471-2407-14-951
48. Yamamura M, Sato Y, Takahashi K, Sasaki M, Harada K. The cyclin-dependent kinase pathway involving CDK1 is a potential therapeutic target for cholangiocarcinoma. *Oncol Rep*. 2019;43(1):306–317. doi:10.3892/or.2019.7405
49. Gavet O, Pines J. Progressive activation of CyclinB1-Cdk1 coordinates entry to mitosis. *Dev Cell*. 2010;18(4):533–543. doi:10.1016/j.devcel.2010.02.013
50. Gavet O, Pines J. Activation of cyclin B1-Cdk1 synchronizes events in the nucleus and the cytoplasm at mitosis. *J Cell Biol*. 2010;189(2):247–259. doi:10.1083/jcb.200909144